

Global warming amplified by reduced sulphur fluxes as a result of ocean acidification

Katharina D. Six^{1*}, Silvia Kloster¹, Tatiana Ilyina¹, Stephen D. Archer^{2,3}, Kai Zhang⁴
and Ernst Maier-Reimer^{1†}

Climate change and decreasing seawater pH (ocean acidification)¹ have widely been considered as uncoupled consequences of the anthropogenic CO₂ perturbation^{2,3}. Recently, experiments in seawater enclosures (mesocosms) showed that concentrations of dimethylsulphide (DMS), a biogenic sulphur compound, were markedly lower in a low-pH environment⁴. Marine DMS emissions are the largest natural source of atmospheric sulphur⁵ and changes in their strength have the potential to alter the Earth's radiation budget⁶. Here we establish observational-based relationships between pH changes and DMS concentrations to estimate changes in future DMS emissions with Earth system model⁷ climate simulations. Global DMS emissions decrease by about 18(±3)% in 2100 compared with pre-industrial times as a result of the combined effects of ocean acidification and climate change. The reduced DMS emissions induce a significant additional radiative forcing, of which 83% is attributed to the impact of ocean acidification, tantamount to an equilibrium temperature response between 0.23 and 0.48 K. Our results indicate that ocean acidification has the potential to exacerbate anthropogenic warming through a mechanism that is not considered at present in projections of future climate change.

Impacts of climate change on marine biology and, thus, initiated potential feedback mechanisms on climate-relevant processes in the atmosphere are considered to be among the greatest unknowns in our understanding of future climate evolutions. Recently, ocean acidification has been identified as a potential source of biologically induced impacts on climate¹. The continuous uptake of anthropogenic carbon dioxide by the oceans changes the chemical composition of the marine environment and lowers the seawater pH. Today's mean surface pH values are already reduced by 0.1 units compared with preindustrial times¹ and future projections for the end of the twenty-first century give local decreases of up to 0.5 units⁸. As marine biota have not been exposed to such drastic pH changes over the past 300 million years⁹, multifarious impacts on biogenic cycles are conceivable.

In mesocosm studies¹⁰ it was observed that DMS, a by-product of phytoplankton production, showed significantly lower concentrations in water with low pH (ref. 4). When DMS is emitted to the atmosphere its oxidation products include gas-phase sulphuric acid, which can condense onto aerosol particles or nucleate to form new particles, impacting cloud condensation nuclei that, in turn, change cloud albedo and longevity¹¹. As oceanic DMS emissions constitute the largest natural source of atmospheric sulphur⁶, changes in DMS could affect the radiative balance and alter the heat budget of the atmosphere¹².

The main focus here is to investigate the climate impact of a decrease in global marine DMS emissions that might result from the exposure of marine biota to significant pH changes induced by ocean acidification. To address this question we apply a series of models. We use the Earth system model (ESM) of the Max Planck Institute for Meteorology⁷ (MPI-ESM), which combines general circulation models of the atmosphere and the ocean. The ocean model comprises a biogeochemical module¹³ that includes a parameterization of the marine sulphur cycle^{14,15} (Methods). The global pattern of present-day simulated DMS concentration of MPI-ESM agrees quite well with an observation-based climatology¹⁶ (Supplementary Fig. S1). Note that in the MPI-ESM, DMS emissions do not have an impact on climate. To quantify the potential climate impact of altered marine sulphur fluxes, we carried out simulations with a standalone version of the atmospheric circulation model that includes sulphur chemistry and aerosol microphysics^{17,18} (Methods).

With the MPI-ESM we run simulations with anthropogenic forcing following the Intergovernmental Panel on Climate Change Special Report on Emissions Scenarios (IPCC SRES) A1B scenario¹⁹ for the period from 1860 to 2100. Model experiments consist of a set of runs including pH-sensitive DMS production and one reference run with no pH-change implications on the marine sulphur cycle (Supplementary Information).

The key function here is the dependence of DMS concentration on seawater pH. In various mesocosm and laboratory microcosm experiments a tendency for decreasing DMS concentrations with decreasing pH has been observed²⁰. In contrast to these findings, one study showed a DMS increase with decreasing pH, which was attributed to an enhanced grazing pressure due to a community shift²⁰. Recent data from a large mesocosm experiment in 2010 in polar waters of Svalbard, Norway, support a DMS decrease in acidified water²¹. To establish functions describing the dependency of the DMS production on pH we average these Svalbard data for the mid-phase after nutrient addition and for the whole period of the experiment (Fig. 1; for details see ref. 21). The DMS concentrations for the mid-phase show, to first order, a linear decrease with lower concentrations of approximately 35(±11%) between a pH range of 8.3 and 7.7 (p_{CO_2} of 190–750 parts per million by volume)²¹. Averaged values for the whole experiment are still 12(±13%) lower for the same pH range. Furthermore, results from mesocosm studies carried out in temperate water of a Norwegian fjord in the years 2003, 2005 and 2006 imply a much stronger sensitivity of DMS concentration on decreasing pH (Fig. 1 and Supplementary Table S1). By basing our approach on the results from mesocosm experiments our intention is to encompass the variety of biological processes that govern net DMS production. Nonetheless, we note that the

¹Max Planck Institute for Meteorology, Bundesstrasse 53, 20146 Hamburg, Germany, ²Plymouth Marine Laboratory, The Hoe, Plymouth PL1 3DH, UK, ³Bigelow Laboratory for Ocean Sciences, 60 Bigelow Dr., PO Box 380, East Boothbay, Maine 04544, USA, ⁴Pacific Northwest National Laboratory, PO Box 999, MSIN K9-24, Richland, Washington 99352, USA. †Deceased. *e-mail: katharina.six@zmaw.de

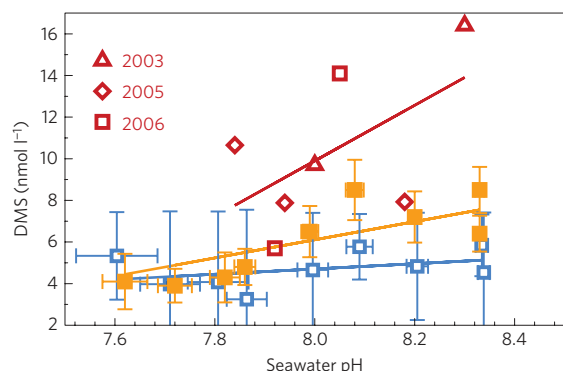


Figure 1 | Relationship between DMS concentration and pH based on data from mesocosm experiments. Measurements of DMS and seawater pH are averaged over the mid-phase of the Svalbard experiment (orange squares) and over the whole experimental period (open blue squares)²¹. Measurements from a mesocosm study in temperate Norwegian waters from three different years are also shown⁴ (open red symbols). The error bars indicate the standard deviation of measurements for DMS and pH. Lines represent linear fits to the data sets of the low- (blue), medium- (orange) and high- (red) pH-sensitive experiment.

level of understanding of the processes behind the response of DMS to ocean acidification is hitherto very poor^{4,21,22}. Furthermore, establishing a consistent response among mesocosm studies is confounded by considerable differences in the experimental set-ups that have been used, including: volumes of seawater enclosed; method used to alter acidity of the sea water; and the stability of the pH values over time (Supplementary Information).

From Fig. 1 we derive a relationship, F , to modify the DMS production rate (Supplementary Equation S2) with $F = 1 + (\text{pH}_{\text{act}} - \text{pH}_{\text{pre}}) \cdot \gamma$. The monthly mean climatological surface pH value, pH_{pre} , was obtained from the first ten years of the reference run (1860–1869) and pH_{act} is the present *in situ* pH value. The multiplicative factor γ denotes the gradient of the linear fit for each data set: the whole Svalbard experiment with a low $\gamma = 0.25$; the mid-phase with a medium $\gamma = 0.58$; the three years measurements in a Norwegian fjord with a high

$\gamma = 0.87$ gradient (Fig. 1). We carry out three studies applying the low, medium and high sensitivity of DMS on pH changes to evaluate the uncertainties underlying our assumption. In the following we focus our discussion on the results for the medium-pH-sensitive experiment.

Annual mean pH_{act} decreases during the simulation following the increase of anthropogenic CO_2 storage in the ocean. The annual mean pH reduction varies regionally between 0.25 and 0.4 units in 2100 as compared with the 1860s (Fig. 2a). Higher latitudes, known to absorb significant amounts of anthropogenic CO_2 , show a stronger pH reduction up to 0.5 units.

Besides a potential pH sensitivity, the main drivers of the marine DMS cycle are the net primary production, or more precisely the decay of organic matter, and the plankton composition (Supplementary Information). Any change to these quantities will directly affect the DMS concentration. We find that the global net primary production and export production of detritus decrease globally by about 16% from 1860 to 2100 (Table 1 and Fig. 2d). These changes are attributed to an increased stratification of the water column due to climate warming, which leads to a reduction in nutrient supply to surface layers²³. In almost all ocean regions a decrease in biological production is projected; only in polar regions does the retreat of sea ice lead to an increased phytoplankton growth and a small increase in net primary and export production (Fig. 2d). The increased water-column stratification also reduces the supply of silicate to the surface layers, which causes a plankton community shift towards calcifiers, that is, towards high-DMS-producing plankton species, in some areas (Supplementary Fig. S2). Globally, the DMS production is decreased by 12% in 2100 in the reference run (Fig. 2b). The reference run and the pH-sensitive runs produce basically the same global patterns and global annual mean fluxes for net primary and export production and result in similar plankton composition because the physical circulation fields are identical (Table 1). In contrast, we find a substantial decrease by 26% in DMS production in the medium-pH-sensitive run by 2100 (Fig. 2e). Even regions in which biological production is projected to increase, such as the Southern Ocean at 60° S, show a reduction in the DMS production due to the significant decrease of seawater pH (Fig. 2a).

Changes in the DMS production are not uniformly transferred to changes in the DMS sea-to-air flux (Fig. 2c,f). The global annual

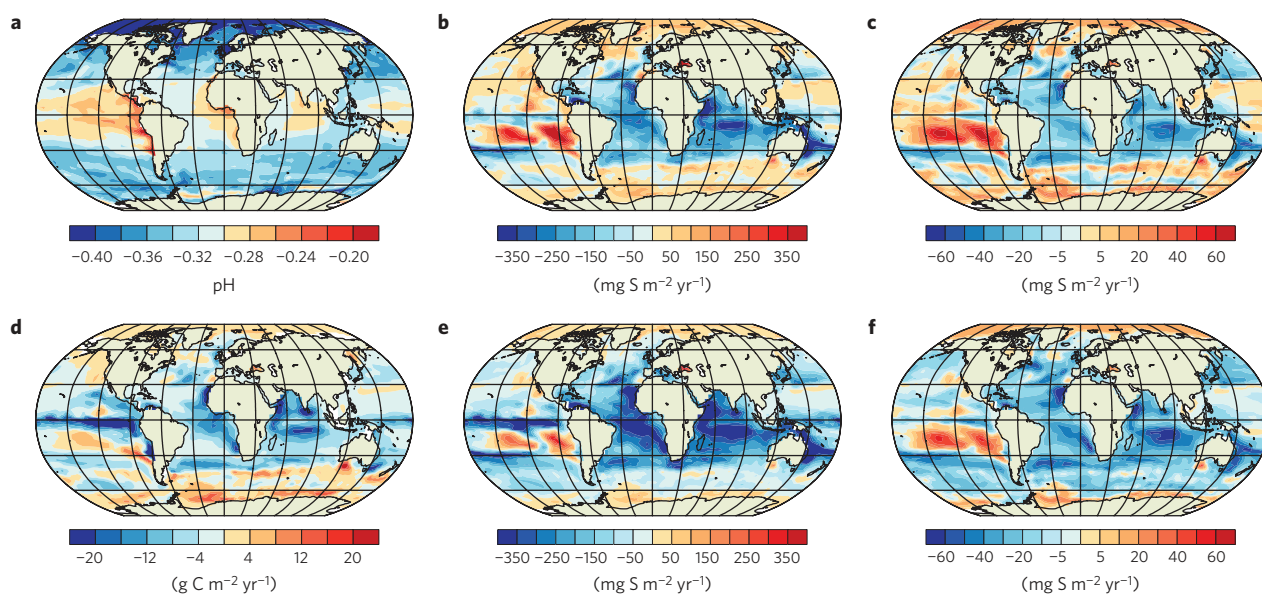


Figure 2 | Changes in annual mean pH and annual mean model fluxes between the years 2090–2099 and 1865–1874. a–f, Surface water pH (a) and export production (d) are shown only for the reference run as the pH-sensitive runs show the same patterns; DMS production for the reference run (b) and the medium-pH-sensitive run (e); DMS flux to the atmosphere for the reference run (c) and the medium-pH-sensitive run (f).

Table 1 | Globally averaged fluxes over the decade 1865–1874 (19th) and the decade 2090–2099 (21st) for the reference and three pH-sensitive runs.

pH impact factor	Unit	Reference run		pH-sensitive runs		
		19th None	21st None	21st Low	21st Medium	21st High
Net primary production	Gt C yr ⁻¹	46	38 (–17%)	38	38	38
Detritus export production	Gt C yr ⁻¹	9.4	7.9 (–16%)	7.9	7.9	7.9
DMS production	Tg S yr ⁻¹	182	160 (–12%)	147 (–18%)	132 (–26%)	118 (–35%)
DMS flux to atmosphere	Tg S yr ⁻¹	29	27 (–7%)	25.5 (–12%)	24 (–17%)	22 (–24%)
Global radiative forcing	W m ⁻²	—	Climate only 0.08	0.18	Ocean acidification–climate 0.40	0.64
Equivalent temperature response	K	—	0.04–0.09	0.1–0.21	0.23–0.48	0.36–0.76

The numbers in brackets are the differences in the carbon or sulphur fluxes between the twenty-first and nineteenth centuries given on a percentage basis. Results for 19th of the pH-sensitive runs are identical to the results of the reference run for 19th. Global radiative forcing and equilibrium temperature response are given as difference between the twenty-first and the nineteenth century. For the pH-sensitive runs, in addition, the climate impact as deduced from the reference run is subtracted.

DMS emissions in the reference run decrease from 29 Tg S to 27 Tg S from 1860 to 2100 representing only a 7% reduction. For the medium-pH-sensitive run the global annual DMS emissions drop from 29 Tg S to 23.8 Tg S (–17%). The low-pH-sensitive experiment results in a 12% and the high one in a 24% decrease in DMS emission; thus, we find a linear response of DMS emission to the change of the multiplicative factor γ (Table 1). The relatively smaller reduction of the DMS emission compared with the DMS production in all experiments can be explained by a shift of high-DMS-producing areas into ocean regions with higher wind speeds, which allows for a more effective DMS gas transfer to the atmosphere.

Incorporating the pH-induced decrease in DMS emissions in a standalone atmospheric circulation model that includes sulphur chemistry and aerosol-cloud microphysics¹⁸ (Methods) leads to a positive global mean top-of-the-atmosphere radiative forcing (Table 1). In the reference run the global radiative forcing is small (0.08 W m⁻²). For the medium-pH-sensitive run a global radiative forcing of 0.48 W m⁻² is simulated. Subtracting the contribution owing to climate change as deduced from the reference run, we get an additional radiative forcing of 0.40 W m⁻² from the impact of pH on DMS. The low- and high-pH-sensitive runs project an additional global radiative forcing of 0.18 and 0.64 W m⁻², respectively. The strongest positive radiative forcing is located in the latitudinal bands around 40° in both hemispheres in areas in which DMS emissions were reduced significantly (Fig. 3 and Supplementary Fig. S3). Consistently, areas with increased DMS emission such as the remote polar oceans show a negative radiative forcing. The subtropical gyre in the South Pacific is also an area with increased DMS emission, but there is no detectable signal in the radiative forcing pattern (Supplementary Fig. S3). This apparent contradiction emphasizes that nonlinear processes associated with aerosol chemistry, cloud microphysics and cloud-dynamical adjustments may play an important role in regulating the climate response to regional DMS emission changes as shown by other model studies^{24,25}.

It is interesting to note that the impact of the pH-induced DMS emission changes on radiative forcing varies little when different anthropogenic background aerosol emissions are applied. We carried out a set of additional runs with a medium pH sensitivity and anthropogenic aerosol emissions, representative of the year 2000 or a Representative Concentration Pathway projection²⁶ for the year 2100. We found a mean radiative forcing of 0.50 ± 0.03 W m⁻² for this set of experiments (Supplementary Information).

Our result of an additional radiative forcing of 0.40 W m⁻² for the medium-pH-sensitive run can be compared with the radiative forcing of 3.71 W m⁻² that is estimated for a CO₂ doubling¹⁹. The significance of our result might become clearer if we convert the

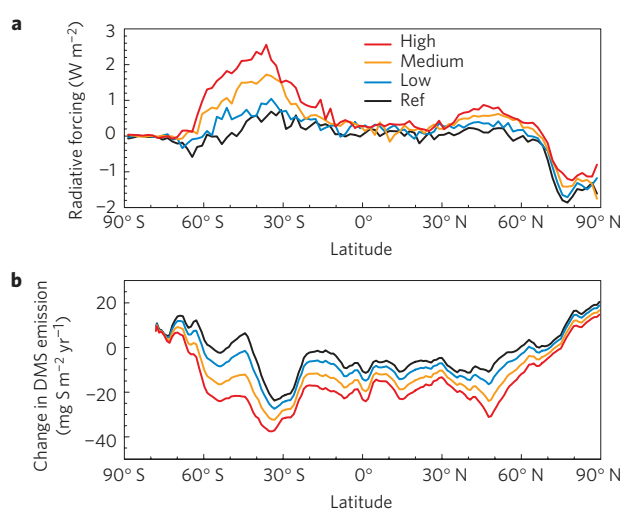


Figure 3 | Changes in annual zonal mean of top-of-the-atmosphere radiative forcing and of DMS emission between the years 2090–2099 and 1865–1874. a, b. The difference in the top-of-the-atmosphere radiative forcing (a) and the change in zonal mean DMS emissions (b). Results are shown for the reference run (Ref) and the three pH-sensitive runs (low, medium and high); see legend in a.

signal into a temperature response: by applying an equilibrium climate sensitivity given for a CO₂ doubling of 2.1–4.4 K (ref. 19) we diagnose an additional equilibrium temperature response between +0.23 and +0.48 K for the medium-pH-sensitive run (from +0.1 to +0.76 K including low and high runs).

To our knowledge we are the first to highlight the potential climate impact due to changes in the global sulphur cycle triggered by ocean acidification. We find that even in a future CO₂ emission scenario as moderate as the IPCC SRES A1B, pH changes in sea water are large enough to significantly reduce marine DMS emissions by the end of the twenty-first century, causing an additional radiative forcing of 0.40 W m⁻². This would be tantamount to a 10% additional increase of the radiative forcing estimated for a doubling of CO₂. Our result emphasizes that this potential climate impact mechanism of ocean acidification should be considered in projections of future climate change. Additional sensitivity experiments show this result varies little with regard to the anthropogenic aerosol background emission. However, a fully coupled transient climate run would be necessary to account for possible feedbacks between ocean acidification and aerosol emissions. Owing to the nonlinear atmospheric response to changes in DMS emissions

the projected temperature increase could be amplified if the Earth system faces a higher CO₂ emission scenario or a higher sensitivity of DMS on pH changes. Furthermore, ocean acidification might additionally have other impacts on marine biota that may provoke further reductions in marine DMS emission²⁷. Progress in understanding the sensitivity of pelagic plankton communities to ocean acidification is required to reduce uncertainties in the effects of non-CO₂ climate-relevant gases in future climate projections.

Methods

We applied an ESM including the marine sulphur cycle to project changes in marine sulphur emission and an atmospheric circulation model with aerosol microphysics to quantify the radiative changes resulting from reduced marine sulphur fluxes. We had to follow a two-step approach as the ESM does not include the calculation of microphysical aerosol processes.

MPI-ESM. Here we briefly summarize the processes within the ocean carbon cycle model (HAMOCC5; ref. 13) that are attributed to the marine DMS cycle^{14,15}. More details of the model are given in the Supplementary Information. The marine DMS cycle comprises production, bacterial consumption, photolysis and gas exchange with the atmosphere. We don't include other biogenic sulphur components such as dimethylsulphoniopropionate or dimethylsulphoxide. Photolysis and DMS gas exchange are linear functions of the DMS concentration. Bacterial consumption is a linear function of temperature and a monod-type saturation function of DMS. We describe the DMS production as a function of detritus export production from silicifiers and calcifiers. The separation into detritus export production from silicifiers and calcifiers credits the fact that haptophytes have, in general, a higher cell ratio of dimethylsulphoniopropionate to carbon and, thus, contribute more to DMS production²⁸. By assigning the DMS production to detritus export production we condense the whole complexity of the biogenic sulphur cycle to its primary driver (phytoplankton) and its final component (DMS).

Atmospheric circulation model with aerosol chemistry ECHAM5.5-HAM2.

The aerosol-climate model ECHAM5.5-HAM2 (refs 17,18) allows us to assess the direct aerosol effect as well as the indirect aerosol effect (owing to changes in cloud properties) caused by changes in DMS emission. The aerosol module HAM2 includes an explicit modal aerosol scheme M7, which considers seven externally and internally mixed lognormal modes and calculates the aerosol processes: nucleation, condensation and coagulation²⁹. Aerosol species considered are sulphate, sea salt, black carbon, organic carbon and mineral dust. We carried out simulations with anthropogenic aerosol emissions for the years 2000 and 2100 (projections from Representative Concentration Pathway scenarios 2.6, 4.5 and 8.5)²⁶ by nudging the model to the ERA-40 reanalysis data for the year 2000. The results presented here are obtained by one-year simulations preceding three-month spin-up periods. As lower marine boundary forcing for the sulphur cycle we used decadal means of the DMS flux (1865–1874 or 2090–2099) from the reference run or from one of the pH-sensitive runs conducted with the MPI-ESM.

Received 18 September 2012; accepted 17 July 2013;
published online 25 August 2013

References

- Gattuso, J.-P. & Hansson, L. in *Ocean Acidification* (eds Gattuso, J.-P. & Hansson, L.) 1–20 (Oxford Univ. Press, 2011).
- Turley, C. *The Other CO₂ Problem* (openDemocracy, 2005); available at: <http://www.acamedia.info/sciences/sciliterature/globalw/reference/carolturley.html>.
- Doney, S. C., Fabry, V. J., Feely, R. A. & Kleypas, J. A. Ocean acidification: The other CO₂ problem. *Annu. Rev. Mar. Sci.* **1**, 169–192 (2009).
- Hopkins, F., Nightingale, P. & Liss, P. in *Ocean Acidification* (eds Gattuso, J.-P. & Hansson, L.) 210–229 (Oxford Univ. Press, 2011).
- Bates, T. S., Lamb, B. K., Guenther, A., Dignon, J. & Stoiber, R. E. Sulfur emissions to the atmosphere from natural sources. *J. Atmos. Chem.* **14**, 315–337 (1992).
- Levasseur, M. If Gaia could talk. *Nature Geosci.* **4**, 351–352 (2011).
- Jungclaus, J. H. *et al.* Climate and carbon-cycle variability over the last millennium. *Clim. Past* **6**, 723–727 (2010).
- Ilyina, T., Zeebe, R. E. & Brewer, P. G. Future ocean increasingly transparent to low-frequency sound owing to carbon dioxide emissions. *Nature Geosci.* **3**, 18–21 (2010).
- Hönisch, B. *et al.* The geological record of ocean acidification. *Science* **335**, 1058–1063 (2012).

- Riebesell, U., Bellerby, R. G. J., Grossart, H.-P. & Thingstad, F. Mesocosm CO₂ perturbation studies: From organism to community level. *Biogeosciences* **5**, 1157–1164 (2008).
- Carlsaw, K. S. *et al.* A review of natural aerosol interactions and feedbacks within the Earth system. *Atmos. Chem. Phys.* **10**, 1701–1737 (2010).
- Charlson, R. J., Lovelock, J. E., Andreae, M. O. & Warren, S. G. Oceanic phytoplankton, atmospheric sulphur, cloud albedo and climate. *Nature* **326**, 655–661 (1987).
- Maier-Reimer, E. *et al.* *The Hamburg Ocean Carbon Cycle Model HAMOCC5.1—Technical Description* (Berichte zur Erdsystemforschung, Vol. 14, Max Planck Institute for Meteorology, 2005); available at <http://www.mpimet.mpg.de>.
- Six, K. D. & Maier-Reimer, E. What controls the oceanic dimethylsulphide (DMS) cycle? A modeling approach. *Glob. Biogeochem. Cycles* **20**, GB4011 (2006).
- Kloster, S. *et al.* DMS cycle in the marine ocean-atmosphere system—a global model study. *Biogeosciences* **3**, 29–51 (2006).
- Lana, A. *et al.* An updated climatology of surface dimethylsulphide concentrations and emission fluxes in the global ocean. *Glob. Biogeochem. Cycles* **25**, GB1004 (2011).
- Stier, P. *et al.* The aerosol-climate model ECHAM5-HAM. *Atmos. Chem. Phys.* **5**, 1125–1156 (2005).
- Zhang, K. *et al.* The global aerosol-climate model ECHAM-HAM, version 2: Sensitivity to improvements in process representations. *Atmos. Chem. Phys.* **12**, 8911–8949 (2012).
- Meehl, G. & Stocker, T. F. in *IPCC Climate Change 2007: The Physical Science Basis* (eds Solomon, S. *et al.*) 1–18 (Cambridge Univ. Press, 2007).
- Arnold, H. E. *et al.* Interacting effects of ocean acidification and warming on growth and DMS-production in the haptophyte coccolithophore *Emiliania huxleyi*. *Glob. Change Biol.* **19**, 1007–1016 (2013).
- Archer, S. D. *et al.* Contrasting responses of DMS and DMSP to ocean acidification in Arctic waters. *Biogeosciences* **10**, 1893–1908 (2013).
- Kim, J.-M. *et al.* Enhanced production of oceanic dimethylsulphide resulting from CO₂-induced grazing activity in a high CO₂ world. *Environ. Sci. Technol.* **44**, 8140–8143 (2010).
- Steinacher, M. *et al.* Projected 21st century decrease in marine productivity: A multi-model analysis. *Biogeosciences* **7**, 979–1005 (2011).
- Thomas, M. *et al.* Rate of non-linearity in DMS aerosol-cloud-climate interactions. *Atmos. Chem. Phys.* **11**, 11175–11183 (2011).
- Woodhouse, M. T., Mann, G. W., Carlsaw, K. S. & Boucher, O. Sensitivity of cloud condensation nuclei to regional changes in dimethyl-sulphide emissions. *Atmos. Chem. Phys.* **13**, 2723–2733 (2013).
- Moss, R. *et al.* The next generation of scenarios for climate change research and assessment. *Nature* **463**, 747–756 (2010).
- Gao, K. S. *et al.* Rising CO₂ and increased light exposure synergistically reduce marine primary productivity. *Nature Clim. Change* **2**, 519–523 (2012).
- Keller, M., Bellows, W. & Guillard, R. in *Biogenic Sulfur in the Environment* (eds Saltzman, E. & Cooper, W.) 167–181 (ACS-Symposium series, 1989).
- Vignati, E., Wilson, J. & Stier, P. M7: An efficient size-resolved aerosol microphysics module for large-scale aerosol transport models. *J. Geophys. Res.* **109**, D22202 (2004).

Acknowledgements

The work of K.D.S. and S.D.A. was financially supported by the EU FP7 project EPOCA (grant no. 211384). This is a contribution to EU FP7 projects COMBINE (grant no. 226520) and CARBOCHANGE (grant no. 264879). K.Z. was supported by the Office of Science of the US Department of Energy as part of the SciDAC programme. We thank I. Stemmler and U. Niemeier for internal review of the original manuscript.

Author contributions

K.D.S. wrote the paper, carried out the experiments with MPI-ESM and analysed the data. S.K. carried out the experiments with ECHAM-HAM2. S.K. and K.Z. analysed the data. Mesocosms data were provided by S.D.A. All authors discussed the results and commented on the manuscript.

Additional information

Supplementary information is available in the [online version of the paper](#). Reprints and permissions information is available online at www.nature.com/reprints. Correspondence and requests for materials should be addressed to K.D.S.

Competing financial interests

The authors declare no competing financial interests.